

Explaining the $t\bar{t}$ forward-backward asymmetry without dijet or flavor anomalies

Zoltan Ligeti,¹ Gustavo Marques Tavares,² and Martin Schmaltz²

¹*Ernest Orlando Lawrence Berkeley National Laboratory, University of California, Berkeley, CA 94720*

²*Physics Department, Boston University, Boston, MA 02215*

We consider new physics explanations of the anomaly in the $t\bar{t}$ forward-backward asymmetry measured at the Tevatron, in the context of flavor conserving models. The recently measured LHC dijet distributions strongly constrain many otherwise viable models. A new scalar particle in the $\bar{\mathbf{3}}$ representation of flavor and color can fit the $t\bar{t}$ asymmetry and cross section data at the Tevatron and avoid both low- and high-energy bounds from flavor physics and the LHC. An s -channel resonance in $uc \rightarrow uc$ scattering at the LHC is predicted to be not far from the current sensitivity. This model also predicts rich top quark physics for the early LHC from decays of the new scalar particles. Single production gives $t\bar{t}j$ signatures with high p_T^{jet} , pair production leads to $t\bar{t}jj$ and 4 jet final states.

I. INTRODUCTION

The unexpectedly large forward-backward asymmetry in the production of $t\bar{t}$ pairs at the Tevatron as observed by CDF $A^{t\bar{t}} = 0.193 \pm 0.069$ [1] and DØ $A^{t\bar{t}} = 0.24 \pm 0.14$ [2] in 2008 generated a lot of interest, because it is significantly higher than the Standard Model (SM) prediction, $A^{t\bar{t}(\text{SM})} \approx 0.06$ [3–6]. One reason for being excited about this measurement is that the top quark is a very sensitive probe of putative new physics at the TeV scale, because of its large mass and coupling to the Higgs. Therefore, one might expect signs of new physics to first show up in top physics. This hope has received a boost by the recent CDF analysis, which showed that the asymmetry arises from $t\bar{t}$ events with high invariant masses [7]

$$\begin{aligned} A^{t\bar{t}}(m_{t\bar{t}} > 450 \text{ GeV}) &= 0.475 \pm 0.114, \\ A^{t\bar{t}}(m_{t\bar{t}} < 450 \text{ GeV}) &= -0.116 \pm 0.153. \end{aligned} \quad (1)$$

The updated DØ result, only available integrated over $m_{t\bar{t}}$, and uncorrected for effects from reconstruction or selection, $A^{t\bar{t}} = 0.08 \pm 0.04$ [8], is consistent with the integrated CDF result, $A^{t\bar{t}} = 0.158 \pm 0.075$ [7]. So is the recent $A^{t\bar{t}} = 0.417 \pm 0.157$ measurement [9] in the dilepton channel, in which the raw asymmetries, binned as in Eq. (1), also support the same trend. The physics responsible for this anomaly may be related to CDF’s high p_T excess in a boosted top search [10]. The large asymmetry at high masses points towards tree-level exchange of a new heavy particle with strong couplings to first and third generation quarks [11–21]. For fits of four-fermion operators to the asymmetry data see [22, 23].

In absence of flavor symmetries, new states at the TeV scale with strong couplings to quarks are severely constrained by the agreement of a vast amount of flavor physics data with the SM (meson-anti-meson mixing, CP violation, rare decays). We are therefore motivated to look for an explanation of the $t\bar{t}$ asymmetry from new states whose couplings (and masses) preserve the full flavor symmetries of the Standard Model quarks along the lines of Refs. [21, 24, 25].

To do so, we classify the new particles not only by their spin and gauge charges, but also by their quantum num-

bers under the flavor symmetries $SU(3)_Q \times SU(3)_U \times SU(3)_D$. Here $SU(3)_Q$ is the set of transformations which rotate the three generations of left-handed quark doublets, Q , and $SU(3)_{U/D}$ transformations rotate the right-handed quark singlets, U/D . For simplicity, and because this leads to the nicest model, we focus on the case where the new states couple only to right-handed up-type quarks.¹ Depending on whether the coupling is to two quarks or to a quark and an anti-quark, the new states have quantum numbers of a “diquark” with baryon number $2/3$ or a “noquark” with baryon number 0 . Under $SU(3)_U$ flavor the new particles must transform in one of the irreducible representations contained in

$$\text{diquark: } \mathbf{3} \otimes \mathbf{3} = \bar{\mathbf{3}} \oplus \mathbf{6}, \quad \text{noquark: } \mathbf{3} \otimes \bar{\mathbf{3}} = \mathbf{1} \oplus \mathbf{8}. \quad (2)$$

With regards to generating an asymmetry, the diquark models are nice because diquarks contribute to $t\bar{t}$ production in the u -channel (see Fig. 1). This new source of top quarks is peaked in the forward direction and can easily produce a large asymmetry. The “noquarks” in the flavor singlet representation are closely related to the extensively discussed axigluons and do not provide a very good fit to the asymmetry data. The main problem is that they are s -channel resonances coupling to up quarks and to top quarks. They would give rise to features in the invariant mass distribution $d\sigma_{t\bar{t}}/dm_{t\bar{t}}$ of $t\bar{t}$ pairs and also of dijets at the Tevatron and the LHC [18]. The case of the $\mathbf{8}$ of flavor is more interesting as it contributes to $t\bar{t}$ production in the t -channel and the s -channel. It is possible to find good fits to both the asymmetry as well as the total $t\bar{t}$ cross section in this case for either light ($M_8 \sim 300 \text{ GeV}$) or heavy ($M_8 \sim 1000 \text{ GeV}$) new states [21]. Data on dijet resonances from the Tevatron [26–28] and SPS [29, 30] rule out flavor universal couplings in the light case. In addition, light spin one particles are associated with gauge symmetries. This would imply at least an approximate

¹ Coupling to up-type quarks is preferred because it accesses the large up-quark parton distribution function, and even $SU(3)_Q$ symmetric couplings to the quark doublets give rise to new flavor violation proportional to CKM matrix elements.

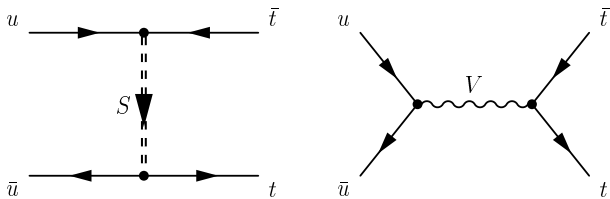


FIG. 1: Feynman diagrams for the new contribution to $u\bar{u} \rightarrow t\bar{t}$ from a diquark (left) and a noquark (right). The flavor symmetry implies an additional t -channel diagram for the noquark **8** (not pictured).

gauge symmetry of flavor, which would need to be broken by the mechanism generating the up-type Yukawa couplings. The heavy state requires very large couplings to generate a large enough asymmetry and can be shown to violate recent bounds on dijets from the LHC [31].² We will not consider the **1** or **8** any further.

Concentrating on renormalizable interactions, the **$\bar{3}$** and **6** must be complex scalar fields and their couplings to quarks can be written as

$$\lambda U^{a\alpha} U^{b\beta} (S^*)^{r\rho} T_{rab} T_{\rho\alpha\beta}. \quad (3)$$

Flavor indices a, b on the quarks run from 1 to 3 and the flavor index on S runs over $r = 1 \dots 3$ or $r = 1 \dots 6$. We also explicitly displayed the color indices $\alpha, \beta = 1 \dots 3$ on the quarks and $\rho = 1 \dots 3$ or $\rho = 1 \dots 6$ on S . Note that the color and flavor quantum numbers of S are correlated, because the two identical quark fields must be symmetric under interchange of color and flavor indices. The scalar **$\bar{3}$** is a $(\bar{3}, 1)_{4/3}$ under the Standard Model gauge group $(SU(3)_c, SU(2)_w)_{U(1)}$ whereas the **6** is a $(6, 1)_{4/3}$. The invariant tensors T are therefore the same for color and flavor. T_{rab} for the **$\bar{3}$** is antisymmetric in a and b whereas for the **6** it is symmetric. We emphasize that in either case these couplings preserve the $SU(3)_U$ flavor symmetry and do not contribute to flavor violating processes.

An obvious but important consequence of the flavor symmetry is that it relates processes involving quarks in different generations. In particular, we observe an important distinction between the **$\bar{3}$** and the **6**. Equation (3) for the **6** contains a coupling of two up quarks to S . This leads to an s -channel resonance in $uu \rightarrow uu$ scattering, which accesses the largest high energy parton luminosities at the LHC and is already severely constrained by recent dijet analyses from CMS [31, 32] and ATLAS [33]. As we will show below, a measurement of dijet angular distributions at CMS [31] already rules out the entire range of couplings and masses for the **6** which generates an appreciable $t\bar{t}$ asymmetry. The **$\bar{3}$** is antisymmetric in its couplings to quarks so that the coupling to two up quarks vanishes.

This leaves the scalar triplet as our only flavor preserving candidate for explaining the $t\bar{t}$ forward-backward asymmetry at the Tevatron. In the following Sections we compare the predictions of this model to all relevant data

1. The binned $t\bar{t}$ asymmetry in Eq. (1) [7];
2. The $p\bar{p} \rightarrow t\bar{t}$ total cross section, $\sigma_{t\bar{t}} = (7.5 \pm 0.48)$ pb [34];
3. Measurement of $d\sigma_{t\bar{t}}/dm_{t\bar{t}}$ [35];
4. The recent CMS dijet analysis [31].

We find that unlike all the other models the triplet scalar is currently unconstrained by dijet data. However, there is some tension between the large $t\bar{t}$ asymmetry required at high invariant masses and the shape of the measured differential cross section as a function of the invariant mass of the $t\bar{t}$ pair. In particular, a 40% asymmetry requires a new physics contribution which is very asymmetric and comparable in size to the $t\bar{t}$ cross section from QCD, but which does not significantly change the shape of the cross section. We are not aware of any model in the literature which completely accomplishes this.

The best fit to the $t\bar{t}$ asymmetry and cross section in our model is obtained for triplet masses in the range 500–800 GeV with relatively large couplings, $\lambda \sim 1.5 - 3.0$ (for even larger couplings our perturbative calculations quickly become suspect). It is therefore easily within reach of the LHC, and both single and pair production of these states should be possible with large cross sections. The most promising processes are single production with top quarks $ug \rightarrow tS_{tu} \rightarrow t\bar{t}j$ and pair production $gg, u\bar{u} \rightarrow SS^* \rightarrow jjjj, t\bar{t}jj$. In the context of flavor-symmetric models it would be particularly interesting if one could measure the forward-backward asymmetries in dijet events with pairs of high p_T charm or bottom quark jets at the Tevatron [18, 36]. Our model predicts an asymmetry for charm quarks similar to that for top quarks and vanishing new physics contribution to the bottom quark asymmetry.

The remainder of the paper is organized as follows. In Section II we define the **$\bar{3}$** and the **6** models, compute the $t\bar{t}$ cross section and asymmetry in each and determine the preferred region in parameter space by fitting to the Tevatron $t\bar{t}$ data. We then compute the predicted dijet rates at the Tevatron and LHC and show that the preferred region of the **$\bar{3}$** model is still allowed whereas the **6** model is ruled out by the CMS dijet measurement. In Section III observable predictions for the LHC from the diquark of the **$\bar{3}$** model are explored.

II. THE **$\bar{3}$** AND THE **6**

The two models contain a new scalar in the **$\bar{3}$** or **6** representation of flavor $SU(3)_U$. The interaction Lagrangian is

$$\mathcal{L} = \lambda U^{a\alpha} U^{b\beta} (S^*)^{r\rho} T_{rab} T_{\rho\alpha\beta} + \text{h.c.}, \quad (4)$$

² The dijet bounds can be evaded with large flavor breaking in the third generation couplings [21].

where Latin (Greek) indices denote flavor (color). The fields U are the right-handed up-type quark singlets with SM charges $(3, 1)_{2/3}$, their Lorentz indices are contracted with $i\sigma_2$. The invariant tensor for the $\bar{\mathbf{3}}$ is $T_{rab} = \epsilon_{rab}/\sqrt{2}$. For the $\mathbf{6}$ the tensor T_{rab} can be decomposed into six 3×3 real symmetric matrices, T_r . In computing amplitudes from exchange of these particles we will use the identities

$$\begin{aligned} (T_3)_{rab} (T_3)^{rcd} &= \frac{1}{2} (\delta_a^c \delta_b^d - \delta_b^c \delta_a^d), \\ (T_6)_{rab} (T_6)^{rcd} &= \frac{1}{2} (\delta_a^c \delta_b^d + \delta_b^c \delta_a^d), \end{aligned} \quad (5)$$

which also fix the normalization of our invariant tensors. Here $T^{rcd} \equiv T_{rcd}^* = T_{rcd}$, because we defined the tensors to be real. Each model has only two parameters, the coupling λ , and the mass m_S . Our definition of the coupling λ differs by a factor of $\sqrt{2}$ in normalization compared to the coupling y of Ref. [13], so that $\lambda = y/\sqrt{2}$. Of course, other viable models may be obtained by including additional free parameters. In the context of minimal flavor violation one might be motivated to consider insertions of $Y_U Y_U^\dagger$. These would have very small effects on light quarks but could change the top quark couplings significantly. We have refrained from doing so in the interest of simplicity and because we expect insertions of $Y_U Y_U^\dagger$ generated from loops to be small.

The process $u(p_1) \bar{u}(p_2) \rightarrow t(k_1) \bar{t}(k_2)$ is given in the SM by s -channel gluon exchange. The S interaction mediates a u -channel contribution (Fig. 1). Including both contributions, the differential partonic cross section is [13–15]

$$\begin{aligned} \frac{d\sigma_{t\bar{t}}}{d\cos\theta} &= \frac{1}{4} \frac{1}{9} \frac{\beta}{2\pi s} \left[g_s^4 \frac{t_t^2 + u_t^2 + 2s m_t^2}{s^2} \right. \\ &\quad \left. + g_s^2 \lambda^2 C_0 \frac{u_t^2 + s m_t^2}{s u_S} + \lambda^4 C_2 \frac{u_t^2}{u_S^2} \right]. \end{aligned} \quad (6)$$

Here θ is the scattering angle between the outgoing top and the incoming quark in the partonic center-of-mass frame, and $\beta \equiv \sqrt{1 - 4m_t^2/s}$. The Mandelstam variables are $s \equiv (p_1 + p_2)^2$, $t \equiv (p_1 - k_1)^2$, $u \equiv (p_1 - k_2)^2$, and we denoted $t_X = t - m_X^2$ and $u_X = u - m_X^2$ ($X = t, S$). Finally, the color factors are $C_0 = 1$ and $C_2 = 3/4$ in the case of the $\bar{\mathbf{3}}$, and $C_0 = -1$ and $C_2 = 3/2$ for the $\mathbf{6}$.³

A. Fitting the $t\bar{t}$ asymmetry at the Tevatron

Our strategy is to fit the models to the $t\bar{t}$ related data from the Tevatron, and then explore whether the resulting parameter space is consistent with other experiments.

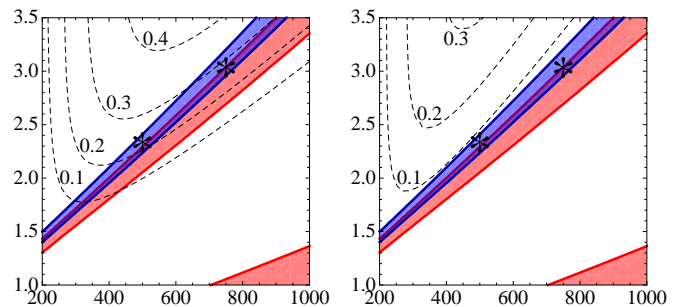


FIG. 2: Regions in m_S vs. λ parameter space for the $\bar{\mathbf{3}}$ model which are allowed by the total cross section constraint. The red (lighter) and blue (darker) shaded regions correspond to $\sigma_{t\bar{t}} - \sigma_{t\bar{t}}^{(\text{SM})} = (0.0 \pm 0.7) \text{ pb}$ and $(1.0 \pm 0.7) \text{ pb}$, respectively. The contours in the left [right] plot show the new physics contribution to the $t\bar{t}$ forward-backward asymmetry $A_{\text{NP}}^{t\bar{t}}(m_{t\bar{t}} > 450 \text{ GeV})$ [$A_{\text{NP}}^{t\bar{t}}(m_{t\bar{t}} < 450 \text{ GeV})$]. The total asymmetry in each bin is obtained by adding the Standard Model contributions, $A_{\text{SM}}^{t\bar{t}} = 0.09$ (left) and 0.04 (right) [7].

We do not perform a χ^2 fit to the data, because the required correlations are not available. One can get a reasonable understanding of the “goodness of fit” of the models by plotting the constraints from various experiments as functions of the models’ two parameters.

In agreement with previous work we find that the well-measured total cross section, $\sigma(p\bar{p} \rightarrow t\bar{t}) = (7.5 \pm 0.48) \text{ pb}$ [34], provides the most important constraint on the parameter space. There is currently some debate in the literature about the precise value of the theoretical prediction. State of the art NLO+NNL [37–39] calculations quote about a 10% uncertainty, and fit the data well. On the other hand, recent calculations resumming threshold logs obtain lower values, around 6.5 pb [40]. Given this uncertainty in the predictions, we choose a conservative approach. We plot the allowed regions corresponding to the central values of each of the theory predictions, with approximately 10% total uncertainties, $\pm 0.7 \text{ pb}$. Thus, the NLO+NNL calculations allow the new physics contribution to the $t\bar{t}$ cross section to account for $\sigma_{t\bar{t}} - \sigma_{t\bar{t}}^{(\text{SM})} = (0.0 \pm 0.7) \text{ pb}$, and yield the red (lighter) shaded allowed regions in Figure 2 for the $\bar{\mathbf{3}}$ model.⁴ Using the threshold resummed predictions, there is additional room for new physics contributions to the $t\bar{t}$ cross section, and the blue (darker) shaded regions show $\sigma_{t\bar{t}} - \sigma_{t\bar{t}}^{(\text{SM})} = (1.0 \pm 0.7) \text{ pb}$. In the former case there are two allowed regions in parameter space. The less interesting region is near the Standard Model and has small Yukawa couplings and therefore small effects

³ Here we note a typographical error in the sign of C_0 for the case of the $\mathbf{6}$ in Ref. [13], which was corrected in Ref. [14].

⁴ In our calculations of the QCD and new physics contributions we applied a K-factor of 1.3. We use the CTEQ-5L parton distribution functions [41] implemented in Mathematica, and checked that MSTW 2008 [42] gives compatible results.

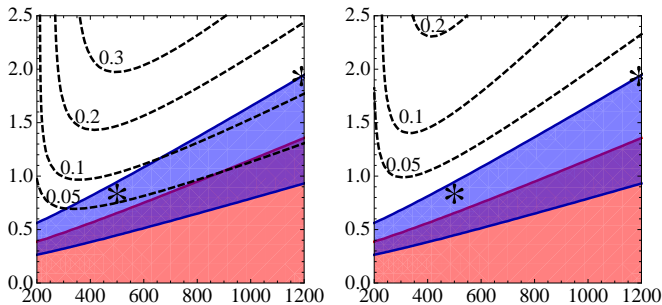


FIG. 3: The contour plots as in Fig. 2, but for the **6** model.

on the forward-backward asymmetry. The regions of interest correspond to narrow bands in parameter space with larger Yukawa couplings. This region is consistent with the total cross section constraint because of a cancellation: the new physics squared contribution to the cross section cancels against the interference with the QCD contribution. Since the total cross section is the most precise of the measurements, the allowed parameter space is largely defined by these narrow bands.

Overlaid on the same plot are contours of constant predicted $t\bar{t}$ forward-backward asymmetry in the high invariant mass bin, $m_{t\bar{t}} > 450$ GeV. One sees that our model can generate parton level $t\bar{t}$ asymmetries between 20% and 30% from the new physics alone. The standard model contributes an additional asymmetry of 0.09 in this bin [7]. To a reasonable approximation the two contributions can simply be added, and the combined asymmetry overlaps the 1σ preferred region of the CDF measurement $A^{t\bar{t}}(m_{t\bar{t}} > 450 \text{ GeV}) = 0.475 \pm 0.10 \pm 0.05$. In the right panel of Fig. 2 we show contours of constant forward-backward asymmetry at low invariant masses, $m_{t\bar{t}} < 450$ GeV, overlaid with the same regions allowed by the total cross section constraint. One sees that even though a large asymmetry of 20–30% is generated at high invariant masses, the asymmetry at low invariant masses is always less than 10% in the region of the parameter space allowed by the total cross section constraint. Based on these “eyeball” fits we define two benchmark points which provide reasonable fits to the CDF asymmetry and total cross section,

- (1) “low mass”: $m_S = 500 \text{ GeV}$, $\lambda = 2.3$,
- (2) “high mass”: $m_S = 750 \text{ GeV}$, $\lambda = 3.0$. (7)

The same fit result for the **6** model is shown in Fig. 3. This model cannot accommodate as high $t\bar{t}$ forward-backward asymmetries as the **3**. Moreover, as discussed below, the dijet constraints already rule it out. For definiteness we also define two benchmark points for this model with $(m_S = 1200 \text{ GeV}, \lambda = 1.9)$ and $(m_S = 500 \text{ GeV}, \lambda = 0.8)$. The two points generate high invariant mass ($m_{t\bar{t}} > 450 \text{ GeV}$) asymmetries of 12% and 6%, respectively.

CDF also provided a binning of the $t\bar{t}$ asymmetry by the rapidity difference between the top anti-top pair. There is a large asymmetry at large rapidity difference and a small asymmetry at small rapidity difference. We find that in our model this binning does not generate new constraints on the parameter space. Our model is consistent with the rapidity binned data within the sizable 1σ errors quoted in Ref. [7].

In Table I we summarize the predictions of the two benchmark points in comparison to the measurements. Our predictions for the asymmetry include both new physics and standard model contributions [7].

Finally, the shape of the $t\bar{t}$ cross section, $d\sigma_{t\bar{t}}/dm_{t\bar{t}}$, has also been measured [35]. The SM prediction for this spectrum is also known at NLO+NNL [37–39]. However, the theoretical uncertainties are larger than for the total cross section, especially at large $m_{t\bar{t}}$ [40]. We do not perform a fit to the spectrum, and only compare the prediction of our model for the cross section in a high invariant mass bin, $700 \text{ GeV} < m_{t\bar{t}} < 800 \text{ GeV}$, following [20]. This bin is fairly far from the bulk of the $t\bar{t}$ data, and therefore tests a different region of the $t\bar{t}$ spectrum than the total cross section. In addition, the cross section at the highest invariant masses is expected to be the most sensitive to the new physics contributions. We find that there is significant tension between the measured cross section and the model prediction for $\sigma_{t\bar{t}} - \sigma_{t\bar{t}}^{(\text{SM})}$ in this bin, with the latter being about twice the SM prediction (a similar excess is found in other models in the literature). Given that both theoretical and experimental uncertainties are substantial for the tail of the $t\bar{t}$ spectrum, we set this issue aside and explore what new information can be obtained from LHC experiments in the context of this model.

B. Dijet constraints

We next study the dijet constraints on the **3** model and contrast them with the corresponding constraints for the **6**. Since the coupling of the **3** in flavor space is $\epsilon_{rab}U^aU^b$ it does not mediate $uu \rightarrow uu$ scattering. This is fortunate because a scalar s -channel resonance of the leading uu parton luminosity with coupling $\lambda > 1$ can be ruled out for masses $\sim 0.4\text{--}3 \text{ TeV}$ with the recent CMS analysis of dijet angular distributions [31]. The **3** model does predict

Observable	Measurement	Point (1)	Point (2)
$A^{t\bar{t}}(m_{t\bar{t}} > 450 \text{ GeV})$	0.475 ± 0.114	0.30	0.36
$A^{t\bar{t}}(m_{t\bar{t}} < 450 \text{ GeV})$	-0.116 ± 0.153	0.10	0.07
$A^{t\bar{t}}(\Delta y \geq 1)$	0.611 ± 0.256	0.42	0.46
$A^{t\bar{t}}(\Delta y < 1)$	0.026 ± 0.118	0.12	0.12
$\sigma_{t\bar{t}} - \sigma_{t\bar{t}}^{(\text{SM})}$	see the text	0.7 pb	0.5 pb

TABLE I: Comparison of the CDF binned asymmetry measurements [7] with the benchmark points in Eq. (7) for the **3** model.

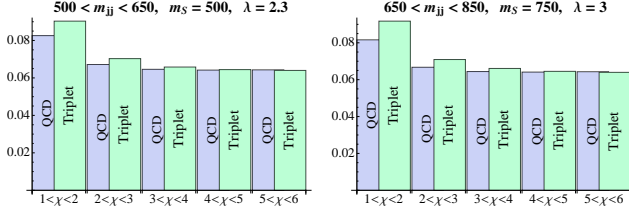


FIG. 4: Normalized dijet cross sections in $\delta\chi = 1$ bins for $1 < \chi < 6$. The blue (darker) histogram shows the QCD prediction, while the green (lighter) histogram shows the normalized sum of QCD and the new physics $uc \rightarrow uc$ contribution to the dijet rate in the $\bar{\mathbf{3}}$ model. The left and right plots show $500 \text{ GeV} < m_{jj} < 650 \text{ GeV}$ and $850 \text{ GeV} < m_{jj} < 1100 \text{ GeV}$, respectively. These are the mass ranges for which the largest excess above QCD is predicted for the two benchmark points (1) and (2) in Eq. (7). In either case the excess in the most central bin is about 10% which is comparable to the uncertainties quoted in [31].

an s -channel dijet resonance in $uc \rightarrow uc$ scattering. As we will see the sensitivity of the CMS analysis is close to what would be required to discover it. The model also gives rise to dijets from u -channel $u\bar{u} \rightarrow c\bar{c}$ processes both at the LHC and at the Tevatron. However, this process is less sensitive than $u\bar{u} \rightarrow t\bar{t}$ or $uc \rightarrow uc$.

The CMS collaboration measured the differential dijet cross section $d\sigma/d\chi$, where $\chi = (1 + |\cos\theta|)/(1 - |\cos\theta|)$ is defined such that it makes the QCD prediction for $d\sigma/d\chi$ flat at small θ . In our models we predict

$$\begin{aligned} \frac{d\sigma}{d\chi} = & \frac{1}{36\pi s(1+\chi)^2} \left[g_s^4 \left(\frac{s^2 + u^2}{t^2} + \frac{s^2 + t^2}{u^2} - \delta \frac{2s^2}{3ut} \right) \right. \\ & + D_0 g_s^2 \lambda^2 \left(\frac{s}{t} + \frac{s}{u} \right) \frac{s(s - m_S^2)}{(s - m_S^2)^2 + m_S^2 \Gamma_S^2} \\ & \left. + 3D_2 \lambda^4 \frac{s^2}{(s - m_S^2)^2 + m_S^2 \Gamma_S^2} \right]. \end{aligned} \quad (8)$$

For $uu \rightarrow uu$ in the $\mathbf{6}$ model we have $\delta = 1$, $D_0 = -2$, and $D_2 = 2$, while for $uc \rightarrow uc$ in the $\bar{\mathbf{3}}$ model $\delta = 0$, $D_0 = 1$, and $D_2 = 1/2$. In both models the width of the resonance is $\Gamma_S = m_S \lambda^2/(8\pi)$. Note that χ does not distinguish between $\pm \cos\theta$, and consequently when computing $d\sigma/d\chi$ for processes where the final state is composed of distinguishable particles, we summed the contributions of both signs of $\cos\theta$.

The CMS analysis contains 9 different dijet invariant mass regions, from 250–350 GeV to above 2.2 TeV. For optimal sensitivity to s -channel new physics beyond the standard model, one looks for a rise in the number of events in the most central bin, $1 < \chi < 2$. QCD predicts an approximately flat distribution over all χ bins with a small rise in the central bin. The measured cross section in each bin is normalized to the total dijet cross section summed over all χ bins. The remaining uncertainty in the central χ bin is estimated by CMS to be about 10% [31].

The scalar resonance in $uc \rightarrow uc$ scattering in the $\bar{\mathbf{3}}$ model does predict an increased dijet rate at

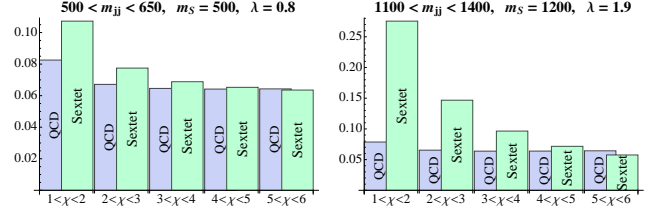


FIG. 5: Same as Fig. 4, but for $uu \rightarrow uu$ in the $\mathbf{6}$ model. The left plot shows the contribution for $500 \text{ GeV} < m_{jj} < 650 \text{ GeV}$, while the right plot shows that for $1100 \text{ GeV} < m_{jj} < 1400 \text{ GeV}$.

small χ , most strongly for dijet invariant masses near m_S . In Fig. 4 we show the predicted normalized dijet rate $(1/\sigma_{\text{dijet}})(d\sigma_{\text{dijet}}/d\chi)$ for our model compared with QCD. For each of the two benchmark points we show the first five χ bins for dijet invariant masses near m_S . There is a discernible rise in the cross section above QCD, but the systematic uncertainties shown in Ref. [31] are of the same size or larger than the new physics effect in Fig. 4. However, increased statistics combined with data driven background subtraction (at higher and lower m_{dijet}) may be sensitive to this uc resonance in the future. If the data starts to show signs of a resonance, it would be very interesting to employ (even limited) charm tagging to confirm the presence of charm quarks.

For comparison, we also show the predicted dijet χ spectrum for the $\mathbf{6}$ model in Fig. 5. Here the resonance is in $uu \rightarrow uu$ scattering, and consequently the new physics signal is very large. We see that the heavy benchmark point for the $\mathbf{6}$ is ruled out by a large margin. The light benchmark point predicts a rise of about 30% beyond QCD which is also ruled out.

C. (Un)Naturalness: SUSY and the Landau pole

Fundamental scalar particles such as our triplet suffer from a naturalness problem, as their masses are quadratically sensitive to ultraviolet scales. Therefore, one should think of this theory as the low energy limit of a more complete theory in which the scalar arises as a composite. Alternatively, the scalar mass may be made natural with supersymmetry. It is straightforward to supersymmetrize our model and we briefly describe the resulting model here.

The minimal supersymmetric version of our model is the MSSM with one extra chiral superfield \bar{S} with identical gauge and flavor quantum numbers as our scalar, and another chiral superfield S with the opposite gauge and flavor quantum numbers. The Yukawa coupling of Eq. (4) is lifted to a superpotential term $W = \lambda UUS$ where now U and S denote the full superfields. Flavor and gauge indices are contracted as in the non-supersymmetric theory. The mass of the scalar gets contributions from supersymmetry breaking and supersymmetry preserving terms. If

it primarily arises from supersymmetry breaking one expects the $S + \bar{S}$ fermions to be light. These fermions are R-parity odd, they can be produced in pairs at the LHC or appear in cascade decays of squarks, giving events with high jet multiplicities and missing energy. The resulting signatures are similar to the ones of a light gluino.

A separate issue the reader may worry about is that the relatively large Yukawa couplings invalidate perturbation theory and lead to a Landau pole not far from the mass of the triplet. The leading term in the beta function for λ is

$$16\pi^2 \frac{d\lambda}{d(\ln \mu)} = 4\lambda^3. \quad (9)$$

We see that there are no large multiplicity factors associated with color and flavor and the loop expansion parameter is approximately $\lambda^2/(4\pi^2)$, which is perturbative for the couplings of interest. The solution to the renormalization group equation is $1/\lambda^2(\mu) = \ln(\Lambda/\mu)/(2\pi^2)$, where Λ is the Landau pole. For example, $\lambda(m_S) = 2.3$ and $m_S = 500$ GeV gives $\Lambda \sim 21$ TeV. (The other benchmark point in Eq. (7), $\lambda(m_S) = 3$ and $m_S = 750$ GeV, gives $\Lambda \sim 7$ TeV.) In either case the Landau pole is far enough that dimension-6 operators suppressed by $16\pi^2/\Lambda^2$ are much smaller than the S exchange diagrams.

III. LHC SIGNALS: uc RESONANCE AND $pp \rightarrow t\bar{t}j$

While $t\bar{t}$ production at the Tevatron is dominated by $q\bar{q} \rightarrow t\bar{t}$, the total $pp \rightarrow t\bar{t}$ cross section at the LHC is dominated by $gg \rightarrow t\bar{t}$, which does not exhibit a forward-backward asymmetry. By measuring $t\bar{t}$ pairs at higher average rapidity or higher invariant mass, one can enhance the $q\bar{q}$ initial state, and thus possibly check the Tevatron observation. Another possibility is to measure the difference of the t and \bar{t} production rates at high rapidity (maybe at LHCb), where one could be sensitive to the asymmetry without reconstructing both the t and the \bar{t} particles in the same event.

Since neither of these measurements are straightforward, it is worthwhile to explore possible other signatures. One exciting possibility is that the colored scalars discussed could manifest themselves in future higher sensitivity dijet analyses. The constraints are already quite powerful for dijet resonances of valence quarks (for example ruling out the **6**). The **3** appears as an s -channel resonance only in $uc \rightarrow uc$ scattering and in the $u\bar{u} \rightarrow c\bar{c}$. Depending on the choice of parameters in our model either of these processes may be observable with increasing statistics, and would be a spectacular discovery, especially if combined with even some limited charm tagging.

Another promising signature, discussed recently in Ref. [43] (in the context of flavor violating models), is to look for $ug \rightarrow S_{ut}\bar{t} \rightarrow t\bar{t}u$ production (see Fig. 6). Since in our preferred scenario $m_S \gg m_t$, the u -quark jet from the decay of S would have high p_T^{jet} , where the standard

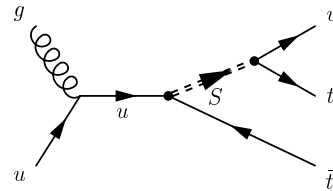


FIG. 6: The flavor conserving diquark contribution to $t\bar{t}j$ production at the LHC. Two other diagrams with the gluon attached to the S and to the \bar{t} are not shown.

model background (known at NLO [44]) is suppressed. The $t\bar{t}j$ cross section from our model would be quite large. For example, at the 7 TeV LHC the new physics contribution is 2 pb for $m_S = 600$ GeV and $\lambda = 1/\sqrt{2}$ (and 7.7 pb for $m_S = 400$ GeV, $\lambda = 1/\sqrt{2}$) [43], and for arbitrary coupling it is enhanced by $2\lambda^2$. Comparing with recent predictions for the $t\bar{t}j$ distributions at the 7 TeV LHC [45, 46], we find that simply cutting on p_T of the hardest jet, our signal is somewhat smaller than the SM background. The experimental sensitivity can probably be optimized and substantially enhanced by measuring the $t\bar{t}j$ rate as a function of both p_T^{jet} and $m_{t\bar{t}}$ (since for the SM background, but not for the signal coming from $\bar{t}S$ decay, p_T^{jet} and $m_{t\bar{t}}$ are anti-correlated), and choosing suitable cuts on both variables.

In addition, pair production of SS^* gives rise to a $t\bar{t}u\bar{u}$ (or $4j$) final state where the unflavored jets have large p_T^{jet} . The rate is smaller than $\bar{t}S$ production, however the second hard jet is advantageous for rejecting SM backgrounds. Especially when the LHC gets to higher energy, the sensitivity in this channel may become competitive with the $t\bar{t}j$ signal.

We conclude that the most promising signals of the **3** at the LHC are either the s -channel resonance contribution whose $uc \rightarrow uc$ origin might become established even with very limited charm tagging, or, especially, $t\bar{t}j$ production at high p_T^{jet} (maybe combined with an $m_{t\bar{t}}$ cut). Without a much more detailed analysis than the present study, it is not possible to determine how the sensitivities of these two searches will compare when the actual experimental analyses are carried out. We hope that both can be pursued by ATLAS and CMS, as they are also interesting searches for models beyond those motivated by the Tevatron $t\bar{t}$ forward-backward asymmetry discussed in this paper.

Note added: The predicted $t\bar{t}$ cross section rises in our model compared to the SM for high invariant masses. For example, the cross section for $m_{t\bar{t}}$ above 1 TeV at the 7 TeV LHC is larger than the QCD cross section by a factor of 2 to 3 in the preferred region of parameter space. Therefore future measurements (combined with improved theory predictions) should discover or rule out our model. Note that the cross section above 1 TeV due to the exchange of a lighter particle cannot be approximated with a higher dimensional operator. Therefore the results of [47, 48] do not apply to our model.

Acknowledgments

We thank Nima Arkani-Hamed, Andy Cohen, Liam Fitzpatrick, Fabio Maltoni, Gilad Perez, David Shih, Brock Tweedie, and Tomer Volansky for helpful conver-

sations. This work was supported in part by the Director, Office of Science, Office of High Energy Physics of the U.S. Department of Energy under contract DE-AC02-05CH11231 (ZL) and DE-FG02-01ER-40676 (MS and GMT).

-
- [1] T. Aaltonen *et al.* [CDF Collaboration], Phys. Rev. Lett. **101**, 202001 (2008) [arXiv:0806.2472 [hep-ex]]; and CDF note 9724, http://www-cdf.fnal.gov/physics/new/top/2009/tprop/Afb/cdfnote_9724_public_v01.pdf.
 - [2] V. M. Abazov *et al.* [D0 Collaboration], Phys. Rev. Lett. **100**, 142002 (2008) [arXiv:0712.0851 [hep-ex]].
 - [3] O. Antunano, J. H. Kuhn and G. Rodrigo, Phys. Rev. D **77**, 014003 (2008) [arXiv:0709.1652 [hep-ph]].
 - [4] M. T. Bowen, S. D. Ellis and D. Rainwater, Phys. Rev. D **73**, 014008 (2006) [arXiv:hep-ph/0509267].
 - [5] J. H. Kuhn and G. Rodrigo, Phys. Rev. D **59**, 054017 (1999) [arXiv:hep-ph/9807420].
 - [6] L. G. Almeida, G. F. Sterman and W. Vogelsang, Phys. Rev. D **78**, 014008 (2008) [arXiv:0805.1885 [hep-ph]].
 - [7] T. Aaltonen *et al.* [CDF Collaboration], arXiv:1101.0034 [hep-ex].
 - [8] DØ Collaboration, DØ Note 6062-CONF, <http://www-d0.fnal.gov/Run2Physics/WWW/results/prelim/TOP/T90/T90.pdf>.
 - [9] CDF Collaboration, CDF note 10398, <http://www-cdf.fnal.gov/physics/new/top/2011/Di1Afb/>.
 - [10] CDF Collaboration, CDF Note 10234, <http://www-cdf.fnal.gov/physics/new/top/2010/tprop/BoostedTops/>.
 - [11] S. Jung, H. Murayama, A. Pierce and J. D. Wells, Phys. Rev. D **81**, 015004 (2010) [arXiv:0907.4112 [hep-ph]].
 - [12] P. H. Frampton, J. Shu, K. Wang, Phys. Lett. **B683**, 294-297 (2010). [arXiv:0911.2955 [hep-ph]].
 - [13] J. Shu, T. M. P. Tait and K. Wang, Phys. Rev. D **81**, 034012 (2010) [arXiv:0911.3237 [hep-ph]].
 - [14] A. Arhrib, R. Benbrik and C. H. Chen, Phys. Rev. D **82**, 034034 (2010) [arXiv:0911.4875 [hep-ph]].
 - [15] I. Dorsner, S. Fajfer, J. F. Kamenik, N. Kosnik, Phys. Rev. **D81**, 055009 (2010). [arXiv:0912.0972 [hep-ph]].
 - [16] G. Burdman, L. de Lima and R. D. Matheus, Phys. Rev. D **83**, 035012 (2011) [arXiv:1011.6380 [hep-ph]].
 - [17] K. Cheung and T. C. Yuan, arXiv:1101.1445 [hep-ph].
 - [18] Y. Bai, J. L. Hewett, J. Kaplan and T. G. Rizzo, arXiv:1101.5203 [hep-ph].
 - [19] J. Shelton and K. M. Zurek, arXiv:1101.5392 [hep-ph].
 - [20] K. Blum *et al.*, arXiv:1102.3133 [hep-ph].
 - [21] B. Grinstein, A. L. Kagan, M. Trott and J. Zupan, arXiv:1102.3374 [hep-ph].
 - [22] C. Degrande, J. M. Gerard, C. Grojean, F. Maltoni and G. Servant, arXiv:1010.6304 [hep-ph].
 - [23] D. W. Jung, P. Ko, J. S. Lee and S. h. Nam, Phys. Lett. B **691**, 238 (2010) [arXiv:0912.1105 [hep-ph]]; arXiv:1012.0102 [hep-ph].
 - [24] C. W. Bauer, Z. Ligeti, M. Schmaltz, J. Thaler and D. G. E. Walker, Phys. Lett. B **690**, 280 (2010) [arXiv:0909.5213 [hep-ph]].
 - [25] J. M. Arnold, M. Pospelov, M. Trott and M. B. Wise, JHEP **1001**, 073 (2010) [arXiv:0911.2225 [hep-ph]].
 - [26] T. Aaltonen *et al.* [CDF Collaboration], Phys. Rev. D **79**, 112002 (2009) [arXiv:0812.4036 [hep-ex]].
 - [27] CDF Collaboration, CDF Note 9609, http://www-cdf.fnal.gov/physics/new/qcd/dijetchi_08/.
 - [28] V. M. Abazov *et al.* [D0 Collaboration], Phys. Rev. Lett. **103**, 191803 (2009) [arXiv:0906.4819 [hep-ex]].
 - [29] G. Arnison *et al.* [UA1 Collaboration], Phys. Lett. B **177**, 244 (1986).
 - [30] J. Alitti *et al.* [UA2 Collaboration], Phys. Lett. B **257**, 232 (1991).
 - [31] V. Khachatryan *et al.* [CMS Collaboration], arXiv:1102.2020 [hep-ex].
 - [32] V. Khachatryan *et al.* [CMS Collaboration], Phys. Rev. Lett. **105**, 211801 (2010) [arXiv:1010.0203 [hep-ex]].
 - [33] G. Aad *et al.* [ATLAS Collaboration], Phys. Lett. B **694**, 327 (2011) [arXiv:1009.5069 [hep-ex]].
 - [34] CDF Collaboration, CDF note 9913, http://www-cdf.fnal.gov/physics/new/top/confNotes/cdf9913_ttbarxs4invfb.ps.
 - [35] T. Aaltonen *et al.* [CDF Collaboration], Phys. Rev. Lett. **102**, 222003 (2009) [arXiv:0903.2850 [hep-ex]].
 - [36] M. J. Strassler, arXiv:1102.0736 [hep-ph].
 - [37] S. Moch and P. Uwer, Phys. Rev. D **78**, 034003 (2008) [arXiv:0804.1476 [hep-ph]].
 - [38] M. Cacciari, S. Frixione, M. L. Mangano, P. Nason and G. Ridolfi, JHEP **0809**, 127 (2008) [arXiv:0804.2800 [hep-ph]].
 - [39] N. Kidonakis and R. Vogt, Phys. Rev. D **78**, 074005 (2008) [arXiv:0805.3844 [hep-ph]].
 - [40] V. Ahrens, A. Ferroglia, M. Neubert, B. D. Pecjak and L. L. Yang, JHEP **1009**, 097 (2010) [arXiv:1003.5827 [hep-ph]]; arXiv:1103.0550 [hep-ph].
 - [41] H. L. Lai *et al.* [CTEQ Collaboration], Eur. Phys. J. **C12**, 375-392 (2000). [hep-ph/9903282].
 - [42] A. D. Martin, W. J. Stirling, R. S. Thorne, G. Watt, Eur. Phys. J. **C63**, 189-285 (2009). [arXiv:0901.0002 [hep-ph]].
 - [43] M. I. Gresham, I. W. Kim and K. M. Zurek, arXiv:1102.0018 [hep-ph].
 - [44] S. Dittmaier, P. Uwer and S. Weinzierl, Eur. Phys. J. C **59**, 625 (2009) [arXiv:0810.0452 [hep-ph]]; S. Dittmaier, P. Uwer and S. Weinzierl, Phys. Rev. Lett. **98**, 262002 (2007) [arXiv:hep-ph/0703120].
 - [45] S. Alioli, Talk at the Heavy Particles at the LHC Workshop, Zurich, 5–7 January 2011, <http://indico.cern.ch/conferenceTimeTable.py?confId=107167#all>.
 - [46] A. Kardos, C. Papadopoulos and Z. Trocsanyi, arXiv:1101.2672 [hep-ph].
 - [47] C. Delaunay, O. Gedalia, Y. Hochberg, G. Perez, Y. Soreq, [arXiv:1103.2297 [hep-ph]].
 - [48] J. A. Aguilar-Saavedra, M. Perez-Victoria, [arXiv:1103.2765 [hep-ph]].